Inorg. Chem. **2006**, *45*, 2184–2192

3-Phenyl-4-benzoyl-5-isoxazolonate Complex of Eu^{3+} with Tri-*n*-octylphosphine Oxide as a Promising Light-Conversion Molecular Device

Rani Pavithran,[†] N. S. Saleesh Kumar,[†] S. Biju,[†] M. L. P. Reddy,*[,†] Severino A. Junior,[‡] and Ricardo O. Freire[‡]

Chemical Sciences and Technology Division, Regional Research Laboratory, CSIR, Thiruvananthapuram 695 019, India, and Departmento de Quimica Fundamental, UFPE, 50 670-901 Recife, PE, Brazil

Received October 14, 2005

Three new europium complexes, $[Eu(PBI)_3 \cdot 3H_2O]$ (**1**), $[Eu(PBI)_3 \cdot 2TOPO]$ (**2**), and $[Eu(PBI)_3 \cdot 2TPPO \cdot H_2O]$ (**3**) (where HPBI, TOPO, and TPPO stand for 3-phenyl-4-benzoyl-5-isoxazolone, tri-*n*-octylphosphine oxide, and triphenylphosphine oxide, respectively), with different neutral ligands were synthesized and characterized by elemental analysis, Fourier transform infrared, ^1H NMR, thermogravimetric analysis, and photoluminescence (PL) spectroscopy. The coordination geometries of the complexes were calculated using the Sparkle/AM1 (Sparkle Model for the Calculation of Lanthanide Complexes within the Austin Model 1) model. The ligand–Eu^{3+} energy-transfer rates were calculated in terms of a model of the intramolecular energy-transfer process in lanthanide coordination compounds reported in the literature. The room-temperature PL spectra of the europium(III) complexes are composed of the typical Eu^{3+} red emission, assigned to transitions between the first excited state ($^5D_0$) and the multiplet ($^7F_{0-4}$). On the basis of emission spectra and lifetimes of the $^5D_0$-emitting level, the emission quantum efficiency (η) was determined. The results clearly show that the substitution of water molecules by TOPO leads to greatly enhanced quantum efficiency (i.e., 26% vs 92%) and longer $^5D_0$ lifetimes (250 vs 1160 μs). This can be ascribed to a more efficient ligand-to-metal energy transfer and a less nonradiative $^5D_0$ relaxation process. Judd–Ofelt intensity parameters (Ω_2 and Ω_4) were determined from the emission spectra for the Eu^{3+} ion based on the $^5D_0 \rightarrow {}^7F_2$ and $^5D_0 \rightarrow {}^7F_4$ electronic transitions, respectively, and the $^5D_0 \rightarrow {}^7F_1$ magnetic-dipole-allowed transition was taken as the reference. A point to be noted in these results is the relatively high value of the Ω_2 intensity parameter for all of the complexes. This may be interpreted as being a consequence of the hypersensitive behavior of the $^5D_0 \rightarrow {}^7F_2$ transition. The dynamic coupling mechanism is, therefore, dominant, indicating that the Eu^{3+} ion is in a highly polarizable chemical environment.

Introduction

Lanthanide complexes have long been known to give sharp and intense emission lines upon ultraviolet light irradiation because of the effective intramolecular energy transfer (ET) from the coordinated ligands to the luminescent central lanthanide ion, which, in turn, undergoes the corresponding radiative process (the so-called antenna effect).[1] Therefore, they are increasingly used as highly efficient electroluminescent components for light-emitting diodes,[2,3] luminescent probes for analytes,[4] labels for proteins and amino acids,[5] and molecular recognition and chirality sensing of biological substrates.[6] The major drawbacks of lanthanides are their low molar extinction coefficients and efficient luminescent quenching by matrix vibrations such as hydroxyl groups via nonradiative pathways, which decreases their luminescence intensity and limits the application for organic light-emitting

* To whom correspondence should be addressed. E-mail: mlpreddy@yahoo.co.uk. Tel: 91-471-2515360. Fax: 91-471-2491712.
[†] CSIR.
[‡] UFPE.

(1) Peng, C.; Zhang, H.; Yu, J.; Meng, Q.; Fu, L.; Li, H.; Sun, L.; Guo, X. *J. Phys. Chem. B* **2005**, *109*, 15278−15287.
(2) Bunzli, J. C. G.; Piguet, C. *Chem. Rev.* **2002**, *102*, 1897−1928.
(3) Kido, J.; Okamoto, Y. *Chem. Rev.* **2002**, *102*, 2357−2368.
(4) Parker, D. *Coord. Chem. Rev.* **2000**, *205*, 109−130.
(5) Yam, V. W. W.; Lo, K. K. W. *Coord. Chem. Rev.* **1999**, *184*, 157−240.
(6) Tsukube, H.; Shinoda, S.; Tamiaki, H. *Coord. Chem. Rev.* **2002**, *226*, 226−227.

10.1021/ic051781d CCC: $33.50
Published on Web 02/01/2006

devices.[7] In addition, because of their low thermal stability, the lanthanide complexes are suitable only for applications in an appropriate temperature range.

A way to circumvent these difficulties is to use ligands bearing suitable chromophores capable of forming thermodynamically stable complexes with lanthanide ions. These ligands could play the antenna role, absorbing light and transferring excitation energy to the emitting ion. Further, when the Ln^{3+} cation is coordinatively unsaturated by the original ligands (β-diketones), an additional neutral ligand coordinates with the metal center to form a highly coordinated complex, thereby excluding the coordination of solvent molecules. Recently, a large number of highly coordinated complexes of lanthanide tris(β-diketonates) containing several nitrogen ligands such as 1,10-phenanthroline,[8] 4,7-disubstituted 1,10-phenanthrolines,[9] 2,2′-bipyridine, 4,4′-disubstituted 2,2′-bipyridines,[9] 1,4-diaza-1,3-butadienes,[10] and 2,2′:6′,6″-terpyridine have been reported.[11,12] The interaction between lanthanide ions and organic ligands and the formation of new complexes with increased coordination number have the effect of protecting metal ions from vibration coupling and increasing their light absorption cross section by the antenna effect.[9] Phosphine oxide ligands in the europium(III) tris(β-diketonate) complex can produce a square antiprismatic structure that promotes faster radiation rates and an increased quantum yield because of an increase in the $^5D_0 \rightarrow {}^7F_2$ emissions (electric dipole transitions), related to odd parity.[13] Furthermore, increased quantum efficiencies of the Eu^{3+} complexes can be expected because coordination of a phosphine oxide molecule prevents coordination of a water or solvent molecule and lowers vibrations. Molecular lanthanide chelates containing 4-acyl-5-pyrazolonate ligands have also been successfully used in the production of emission layers in organic electroluminescent devices.[14] However, another novel class of heterocyclic β-diketones such as 3-phenyl-4-aroyl-5-isoxazolones has not been utilized for the preparation of luminescent materials even though they are well-known as potential complexing agents for lanthanides.[15] Herein, we report the synthesis and photophysical properties of new europium(III) complexes of 3-phenyl-4-benzoyl-5-isoxazolone (HPBI) with Lewis bases such as tri-*n*-octylphosphine oxide (TOPO) or triphenylphosphine oxide (TPPO) (Chart 1).

Chart 1. Molecular Structures of the Ligands

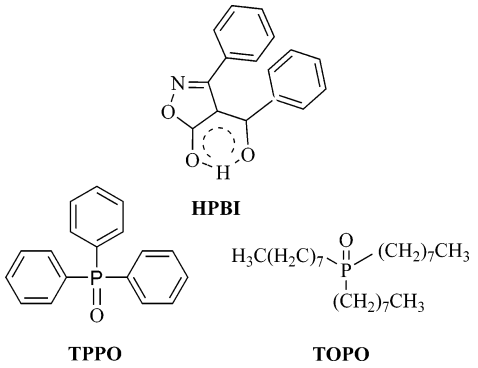

Scheme 1. Synthesis Route of the HPBI

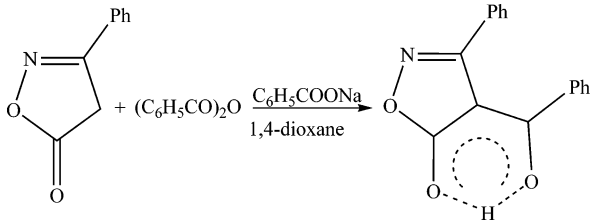

Experimental Section

Commercially available chemicals europium(III) nitrate hexahydrate (99.9%; Acros Organics), 3-phenyl-5-isoxazolone (98%; Aldrich), benzoic anhydride (98%; Aldrich), sodium benzoate, TOPO (99%; Aldrich), and TPPO (98%; Aldrich) were used without further purification. All of the other chemicals used were of analytical reagent grade.

Elemental analyses were performed with a Perkin-Elmer series 2 elemental analyzer 2400. A Nicolet FT-IR 560 Magna spectrometer using KBr (neat) was used to obtain IR spectral data, and a Bruker 300-MHz NMR spectrometer was used to obtain ^{1}H NMR spectra of the compounds in $CDCl_3$ or acetone-d_6 media. Thermogravimetric analyses were carried out using a TGA-50H (Shimadzu, Tokyo, Japan). Photoluminescence (PL) spectra were recorded using a Spex-Fluorolog DM3000F spectrofluorometer with a double-grating 0.22-m Spex 1680 monochromator and a 450-W Xe lamp as the excitation source using the front-face mode. The lifetime measurements were carried out at room temperature using a Spex 1934 D phosphorimeter.

Synthesis of 3-Phenyl-4-benzoyl-5-isoxazolone (HPBI). A mixture of 3-phenyl-5-isoxazolone (3 g, 18 mmol), benzoic anhydride (4.25 g, 18 mmol), and sodium benzoate (4.95 g, 34 mmol) was refluxed in dry 1,4-dioxane (90 mL; Scheme 1) for 3 h. The crude product was filtered, dried, and recrystallized from ethyl acetate.

The synthesized HPBI was identified by elemental analyses and IR and ^{1}H NMR spectral data. Mp: 146 °C. ^{1}H NMR (360 MHz, $CDCl_3$, TMS) ppm: 6.94−8.06 (m, 10H, phenyl). In the ^{1}H NMR spectrum of HPBI, the peak observed at δ 5.90 corresponds to the enolic −OH in the compound, which was found to have exchanged upon the addition of D_2O. IR (KBr) ν_{max}: 3052, 1699, 1613, 1489, 831 cm^{-1}. CHN anal. Calcd for $C_{16}H_{11}NO_3$: C, 72.45; H, 4.15; N, 5.28. Found: C, 72.27; H, 4.18; N, 5.17.

Synthesis of [Eu(PBI)$_3$·3H$_2$O] (1). An aqueous solution of Eu$(NO_3)_3$·6H_2O (0.5 mmol) was added to a solution of HPBI (1.5 mmol) in ethanol in the presence of NaOH (1.5 mmol). Precipitation takes place immediately, and the reaction mixture was stirred for 10 h at room temperature (Scheme 2). It was filtered, washed with ethanol, water, and then ethanol, dried, and stored in a desiccator.

(7) Li, S.; Zhong, G.; Zhu, W.; Li, F.; Pan, J.; Huang, W.; Tian, H. *J. Mater. Chem.* **2005**, *15*, 3221−3228.
(8) de Sa, G. F.; Malta, O. L.; de Mello Donega, C.; Simas, A. M.; Longo, R. L.; Santa-Cruz, P. A.; da Silva, E. F., Jr. *Coord. Chem. Rev.* **2000**, *196*, 165−195.
(9) Bellusci, A.; Barberio, G.; Crispini, A.; Ghedini, M.; La Deda, M.; Pucci, D. *Inorg. Chem.* **2005**, *44*, 1818−1825.
(10) Fernandes, J. A.; Ferreira, R. A. S.; Pillinger, M.; Carlos, L. D.; Goncalves, I. S.; Ribeiro-Claro, P. J. A. *Eur. J. Inorg. Chem.* **2004**, 3913−3919.
(11) Fukuda, Y.; Nakao, A.; Hiyashi, K. *J. Chem. Soc., Dalton Trans.* **2002**, 527−533.
(12) Cotton, S. A.; Noy, O. E.; Liesener, F.; Raithby, P. R. *Inorg. Chim. Acta* **2003**, *344*, 37−42.
(13) Hasegawa, Y.; Yamamuro, M.; Wada, Y.; Kanehisa, N.; Kai, Y.; Yanagida, S. *J. Phys. Chem. A* **2003**, *107*, 1697−1702.
(14) Xin, H.; Shi, M.; Gao, X. C.; Huang, Y. Y.; Gong, Z. L.; Nie, D. B.; Cao, H.; Bian, Z. Q.; Li, F. Y.; Huang, C. H. *J. Phys. Chem. B* **2004**, *108*, 10796−10800.
(15) Pavithran, R.; Reddy, M. L. P. *Radiochim. Acta* **2004**, *92*, 31−38.

Scheme 2. Synthesis Route of the Complex $Eu(PBI)_3 \cdot 3H_2O$

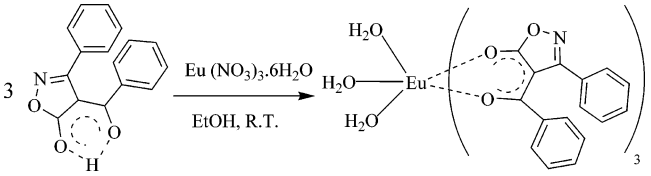

Scheme 3. Synthesis Route of the Complexes $Eu(PBI)_3 \cdot 2TOPO$ and $Eu(PBI)_3 \cdot 2TPPO \cdot H_2O$

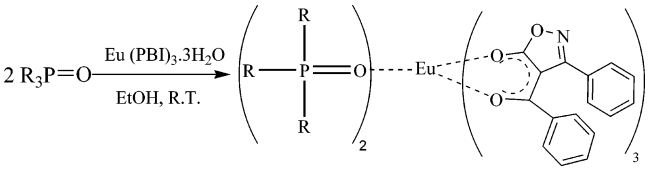

CHN anal. Calcd for $C_{48}H_{36}EuN_3O_{12}$ (997.965): C, 57.72; H, 3.61; N, 4.21; Eu, 15.22. Found: C, 57.52; H, 3.08; N, 4.4; Eu, 15.10. IR (KBr) ν_{max}: 3300, 1641, 1605, 1483, 1389, 1184, 910, 760 cm^{-1}. ^1H NMR (360 MHz, $CDCl_3$, TMS) ppm: 5.07−6.97.

Synthesis of [Eu(PBI)$_3$·2TOPO] (2). An aqueous solution of $Eu(NO_3)_3 \cdot 6H_2O$ (0.5 mmol) was added to a mixture of HPBI (1.5 mmol) in ethanol and TOPO (1.0 mmol) in the presence of NaOH (1.5 mmol). Precipitation takes place immediately, and the reaction mixture was stirred at room temperature (Scheme 3) for 10 h. It was filtered, washed with ethanol, water, and then ethanol, dried, and stored in a desiccator. CHN anal. Calcd for $C_{96}H_{132}EuN_3O_{11}P_2$ (1717.265): C, 67.08; H, 7.69; N, 2.44; Eu, 8.85. Found: C, 67.57; H, 7.58; N, 2.67; Eu, 8.70. IR (KBr) ν_{max}: 2926, 2856, 1651, 1612, 1576, 1493, 1385, 1134, 908, 770 cm^{-1}.

Synthesis of [Eu(PBI)$_3$·2TPPO·H$_2$O] (3). An aqueous solution of $Eu(NO_3)_3 \cdot 6H_2O$ (0.25 mmol) was added to a mixture of HPBI (0.75 mmol) and TPPO (0.5 mmol) in ethanol in the presence of NaOH (0.75 mmol). Precipitation takes place immediately, and the reaction mixture was stirred at room temperature (Scheme 3) for 10 h. It was filtered, washed with ethanol, water, and then ethanol, dried, and stored in a desiccator. CHN anal. Calcd for $C_{84}H_{62}EuN_3P_2O_{12}$ (1518.545): C, 66.38; H, 4.08; N, 2.76; Eu, 10.01. Found: C, 66.40; H, 4.34; N, 3.36; Eu, 9.95. IR (KBr) ν_{max}: 3200, 1651, 1601, 1495, 1391, 1163, 906, 760 cm^{-1}.

Theoretical Approach

Sparkle Model Geometries. The ground-state geometries of all Eu^{3+} complexes were calculated with the new version of the Sparkle/AM1 model[16] implemented in the MOPAC93r2 package.[17] The MOPAC keywords used in all Sparkle/AM1 calculations were as follows: GNORM = 0.25, SCFCRT = 1.D-10 (in order to increase the self-consistent-field convergence criterion), and XYZ (the geometry optimizations were performed in Cartesian coordinates). Recently, Freire et al.[16] have improved the Sparkle model by presenting a much more accurate parametrization. This new parametrization, named Sparkle/AM1, yielded an unsigned mean error for all interatomic distances between the Eu^{3+} ion and the ligand atoms of the first sphere of coordination for 96 different Eu^{3+} complexes of 0.09 Å, an improvement over the value of 0.28 Å for the second version, SMLCII,[18] and the value of 0.68 Å for the original version, SMLC.[19]

INDO/S-CI Electronic Structures. For all calculated ground-state geometries, we have predicted their singlet and triplet excited states using the intermediate neglect of differential overlap/spectroscopic-configuration interaction (INDO/S-CI) method[20,21] implemented in the ZINDO program.[22] We have used a point charge of +3e to represent the trivalent europium ion. The CIS space was gradually increased until there were no further meaningful changes in the calculated transitions. In contrast, the energy levels of the Eu^{3+} metal ions were considered as being those of the free ion in the intermediate coupling scheme.[23] The INDO/S accuracy is about 1000 cm^{-1}.[20]

ET Rates. According to the theoretical model developed by Malta et al.,[24,25] the following expression has been obtained for the ligand−lanthanide ion ET rate, W_{ET} (eq 1).

$$W_{ET} = W_{ET}^{mm} + W_{ET}^{em} \quad (1)$$

The first term, W_{ET}^{mm}, corresponds to the ET rate obtained from the multipolar mechanism (eqs 2 and 3),

$$W_{ET}^{mm} = W_{ET}^{mp} + W_{ET}^{dd} \quad (2)$$

where

$$W_{ET}^{mp} = \frac{2\pi}{\hbar}\frac{e^2 S_L}{(2J+1)G} F \sum_{\lambda} \gamma_{\lambda} \langle \alpha' J' || U^{(\lambda)} || \alpha J \rangle^2 \quad (3)$$

corresponding to the dipole−2^{λ} pole mechanism (λ = 2, 4, and 6), and eq 4

$$W_{ET}^{dd} = \frac{4\pi}{\hbar}\frac{e^2 S_L}{(2J+1)GR_L^6} F \sum_{\lambda} \Omega_{\lambda}^{ed} \langle \alpha' J' || U^{(\lambda)} || \alpha J \rangle^2 \quad (4)$$

corresponding to the dipole−dipole mechanism (λ = 2, 4, and 6).

The second term of eq 1, W_{ET}^{em}, corresponds to the ET rate obtained from the exchange mechanism. This term is calculated from eq 5.

$$W_{ET}^{em} = \frac{8\pi}{3\hbar}\frac{e^2(1-\sigma_0)^2}{(2J+1)R_L^4} F \langle \alpha' J' || S || \alpha J \rangle^2 \sum_m \left| \langle \phi | \sum_k \mu_z(k)\, s_m(k) | \phi' \rangle \right|^2 \quad (5)$$

(16) Freire, R. O.; Rocha, G. B.; Simas, A. M. *Inorg. Chem.* **2005**, *44*, 3299−3310.
(17) Stewart, J. J. P. *MOPAC 93.00 Manual*; Fujitsu Ltd.: Tokyo, Japan, 1993.
(18) Rocha, G. B.; Freire, R. O.; da Costa, N. B., Jr.; de Sa, G. F.; Simas, A. M. *Inorg. Chem.* **2004**, *4*, 2346−2354.
(19) Andrade, A. V. M.; da Costa, N. B., Jr.; Simas, A. M.; de Sa, G. F. *Chem. Phys. Lett.* **1994**, *227*, 349−353.
(20) Ridley, J. E.; Zerner, M. C. *Theor. Chim. Acta* **1976**, *42*, 223−236.
(21) Zerner, M. C.; Loew, G. H.; Kirchner, R. F.; Mueller-Westerhoff, U. T. *J. Am. Chem. Soc.* **1980**, *102*, 589−599.
(22) Zerner, M. C. *ZINDO Manual*; QTP, University of Florida: Gainesville, FL, 1990.
(23) Carnall, W. T.; Crosswhite, H. M. *Energy levels, Structure and Transition Probabilities of the Trivalent Lanthanides in LaF3*; Argonne National Laboratory: Argonne, IL, 1977.
(24) Malta, O. L.; Gonçalves e Silva, F. R. *Spectrochim. Acta A* **1998**, *54*, 1593−1599.

In the above equations, J represents the total angular momentum quantum number of the lanthanide ion, G is the degeneracy of the ligand initial state, α specifies a given 4f spectroscopic term, and S_L is the electric dipole strength associated with the $\phi \rightarrow \phi'$ transition in the ligand. The quantities are reduced matrix elements $U^{(\lambda)}$, and R_L is the distance from the lanthanide ion nucleus to the region of the ligand molecule in which the ligand donor (or acceptor) state is localized. In eq 3, S is the total spin operator of the lanthanide ion, μ_z is the z component of the electric dipole operator and s_m ($m = 0, \pm 1$) is a spherical component of the spin operator, both for the ligand electrons, and σ_0 is a distance-dependent screening factor.

The quantities F and γ_λ are given by eqs 6 and 7, where

$$F = \frac{1}{\hbar\gamma_L}\sqrt{\frac{\ln 2}{\pi}}\exp\left[-\left(\frac{\Delta}{\hbar\gamma_L}\right)^2 \ln 2\right] \quad (6)$$

$$\gamma_\lambda = (\lambda + 1)\frac{\langle r^\lambda\rangle^2}{(R_L^{\lambda+2})^2}\langle 3||C^{(\lambda)}||3\rangle^2(1 - \sigma_\lambda)^2 \quad (7)$$

γ_L is the ligand-state bandwidth at half-height, Δ is the difference between the donor and acceptor transition energies involved in the transfer process, $\langle r^\lambda\rangle$ is the radial expectation value of r^λ for 4f electrons, $\langle 3||\mathbf{C}^{(\lambda)}||3\rangle$ is a reduced matrix element of the Racah tensor operator $\mathbf{C}^{(\lambda)}$,[26] and the σ_λ's are screening factors due to the 5s- and 5p-filled subshells of the lanthanide ion. The selection rules that can be derived from the above equations are the following: $J + J' \geq \lambda \geq |J - J'|$, for the mechanisms expressed by eqs 1 and 2, and $\Delta J = 0$ and ± 1, for the exchange mechanism; in both cases, $J' = J = 0$ is excluded. From the ligand side, the selection rules can be derived from the electric dipole strength S_L and the matrix element of the coupled operators μ_z and S_m in eq 3. The theoretical procedures for using the above equations and the corresponding selection rules have been discussed in detail elsewhere.[27]

Results and Discussion

Syntheses and Characterization of Complexes 1−3. The whole synthetic procedure of europium complexes **1**−**3** is shown in Schemes 2 and 3. The ligand HPBI was synthesized according to the method described in Scheme 1. The microanalyses of complexes **1**−**3** show that the Eu^{3+} ion has reacted with HPBI in a metal-to-ligand mole ratio of 1:3 and two molecules of phosphine oxide are involved in complexes **2** and **3**. The IR spectrum of complex **1** shows a broad absorption in the region of 3000−3500 cm^{-1}, indicating the presence of H_2O molecules in the complex. The existence of water molecules in lanthanide complexes with heterocyclic β-diketones such as 1-phenyl-3-methyl-4-acylpyrazolones is well documented.[28,29] The presence of water molecules was also noticed in complex **3**. The disappearance of the broad band in the region of 3000−3500 cm^{-1} for complex **2**, which is associated with the coordinated water molecules in neat complex **1**, suggests that water molecules have been displaced by the insertion of TOPO as a coordinating unit. The carbonyl stretching frequency of HPBI (1699 cm^{-1}) has been shifted to lower wavenumbers in complexes **1**−**3** (1641 cm^{-1} in **1**, 1651 cm^{-1} in **2**, and 1651 cm^{-1} in **3**), indicating the involvement of carbonyl oxygen in the complex formation with the Eu^{3+} ion. Further, shifts in the P═O stretching frequencies of phosphine oxide molecules in complexes **2** (from 1143 to 1134 cm^{-1}) and **3** (from 1182 to 1163 cm^{-1}) show the involvement of phosphoryl oxygen in the complex formation with the Eu^{3+} ion.

It is clear from the thermogravimetric analysis data that complexes **1** and **3** undergo a mass loss (found, 5.4 and 1.0%; calcd, 5.4 and 1.18%; respectively for complexes **1** and **3**) up to 200 °C, which corresponds to the removal of coordinated water molecules. On the other hand, complex **2** does not undergo any mass loss up to 250 °C, indicating the absence of water molecules in the coordination sphere. Further, decomposition takes place in the region of 250−600 °C for all of the complexes.

The ^{1}H NMR spectrum of complex **1** showed all expected signals for HPBI protons. The integration of the bands was in accordance with the formula proposed. A clear indication of the complex formation is given by the absence of the enolic −OH peak, present in the free ligand, HPBI. Signals for water protons were also noticed in complex **1**, as evidenced from the IR spectral data. The signals of phenyl protons have been shifted upfield upon coordination with the metal ion in the complex (from 6.94−8.06 ppm in HPBI to 5.07−6.97 ppm in **1**).

Molecular Structures of Complexes 1−3 by the Sparkle/AM1 Model. Figures 1−3 show the optimized molecular structures of the europium(III) complexes **1**−**3** obtained using the Sparkle/AM1 model. In complexes **1** and **3**, the Eu^{3+} ion is nine-coordinated and the coordination polyhedron can be approximately described as tricapped trigonal-prismatic geometry. On the other hand, in complex **2**, the Eu^{3+} ion is eight-coordinated and the geometrical structure is determined to be an antisymmetrical square antiprism from the coordination site angles. A similar geometrical structure was reported elsewhere for the tris(hexafluoroacetylacetonate)europium(III) phosphine oxide complex by single-crystal X-ray diffraction.[13]

The tris(β-diketonates) are usually coordinatively unsaturated and therefore readily form adducts with Lewis bases, giving seven-, eight-, or even nine-coordinated complexes.[30,31] In complex **2**, the introduction of a highly basic

(25) Malta, O. L.; Silva, F. R. G.; Longo, R. *Chem. Phys. Lett.* **1999**, *307*, 518−526.
(26) Judd, B. R. *Operator Techniques in Atomic Spectroscopy*, 2nd ed.; McGraw-Hill Book Co.: New York, 1998.
(27) Malta, O. L.; Brito, H. F.; Menezes, J. F. S.; Gonçalves e Silva, F. R.; Alves, S., Jr.; Farias, F. S., Jr.; de Andrade, A. M. V. *J. Lumin.* **1997**, *75*, 255−268.
(28) Pettinari, C.; Marchetti, F.; Cingolann, A.; Drozdov, A.; Timokhin, I.; Troyanov, S. I.; Tsaryuk, V.; Zolin, V. *Inorg. Chim. Acta* **2004**, *357*, 4181−4190.
(29) Zhou, D.; Li, Q.; Huang, C. H.; Yao, G.; Umetani, S.; Matsui, M.; Ying, L.; Yu, A.; Zhao, X. *Polyhedron* **1997**, *16*, 1381−1389.
(30) Amine, S.; Botta, M.; Fasano, M.; Terreno, E. *Chem. Soc. Rev.* **1998**, *27*, 19−29.
(31) Hart, F. A. In *Comprehensive Coordination Chemistry*; Wilkinson, G., Gillard, R. D., McCleverty, J. A., Eds.; Pergamon Press: Oxford, U.K., 1987; Vol. 3, pp 1059−1126.

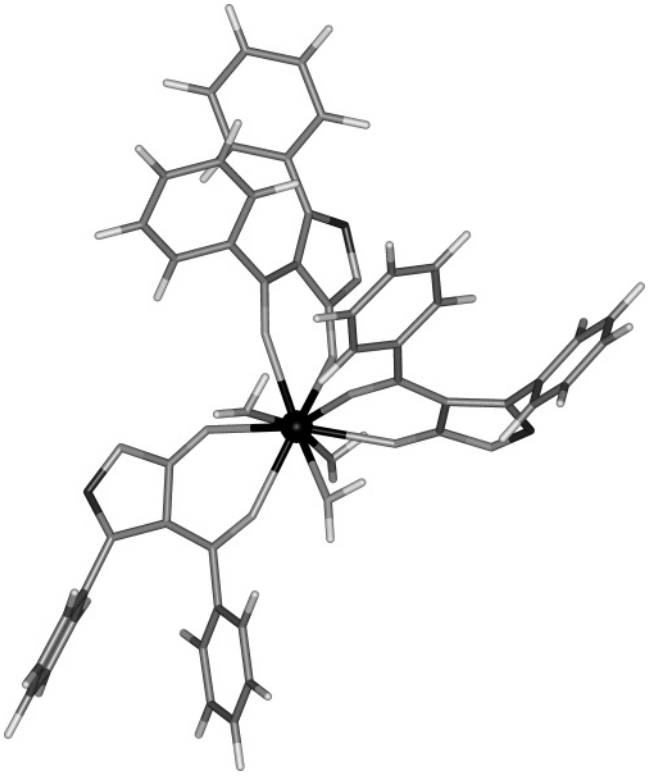

Figure 1. Optimized molecular structure of complex **1** obtained from the Sparkle/AM1 model.

auxiliary ligand such as TOPO [K_H value = 8.9; $H^+(aq) + NO^-_3(aq) + S_{org} \overset{K_H}{\rightleftharpoons} HNO_3 \cdot S_{org}$, where K_H is the nitric acid uptake constant[32]) replaces all of the water molecules from the coordination sphere of the Eu^{3+} ion. On the other hand, in complex **3**, the insertion of weakly basic TPPO (K_H value = 2.3) is not strong enough to replace all of the water molecules present in the coordination sphere.

The spherical coordinates of the bonded oxygens with respect to a coordinate system centered around the Eu^{3+} ion are given in Table 1. These structural data are consistent with a very low symmetry of the chemical environment around the Eu^{3+} ion. An interesting point that is predicted by the present structural optimization is that TOPO and TPPO oxygens are considerably closer to the Eu^{3+} ion than the H_2O oxygen atoms in the case of the hydrated compound **1**. Further, the two Eu−O bonds with TOPO ligands (2.33 and 2.32 Å) and TPPO ligands (2.33 and 2.33 Å) were shorter than the six Eu−O bonds with HPBI ligands (2.39−2.42 Å), as observed in the X-ray single-crystal data (Eu−O bonds with TPPO ligands, 2.32−2.33 Å; Eu−O bonds with hexafluoroacetylacetone ligand, 2.39−2.44 Å) of the complex tris(hexafluoroacetylacetonato)europium(III) with phosphine oxide.[13] This clearly highlights that phosphine oxide ligands interact more strongly with the Eu^{3+} ion in complexes **2** and **3**.

PL Properties of Complexes 1−3. Figure 4 presents the normalized excitation spectra of the europium complexes **1**−**3** at room temperature. The excitation spectra of the complexes were obtained by monitoring the emission wavelength of the Eu^{3+} ions at 612 nm. The excitation spectra of the complexes exhibit a broad excitation band between 250 and 425 nm (λ_{max} = 367 nm), which can be assigned to $\pi-\pi^*$-electron transition of the ligands. A peak at 464 nm is observed as a result of the f−f absorption transition ($^7F_0 \rightarrow {}^5D_2$) of the Eu^{3+} ion. This transition is weaker than the absorption of the organic ligands and is overlapped by a broad excitation band, which proves that luminescence sensitization via excitation of the ligand is much more efficient than the direct excitation of the Eu^{3+} ion absorption level.

The room-temperature normalized emission spectra of europium complexes **1**−**3** (in the solid states) under the excitation wavelength (360 nm) that maximizes the Eu^{3+} emission intensity are shown in Figure 5. The emission spectra of the complexes display characteristic sharp peaks in the 575−725-nm region associated with the $^5D_0 \rightarrow {}^7F_J$ transitions of the Eu^{3+} ion. The five expected peaks of the $^5D_0 \rightarrow {}^7F_{0-4}$ transitions are well resolved, and the hypersensitive $^5D_0 \rightarrow {}^7F_2$ transition is very intense, pointing to a highly polarizable chemical environment around the Eu^{3+} ion, and is responsible for the brilliant-red emission color of these complexes.[33] Further, the emission spectra of the complexes show only one peak for the $^5D_0 \rightarrow {}^7F_0$ transition, indicating the presence of a single chemical environment around the Eu^{3+} ion and also showing that the Eu^{3+} ion occupies a low-symmetry site. No emission band at 525 nm, corresponding to the emission from the lowest triplet state

Table 1. Spherical Coordinates of the Oxygen Atoms Bonded to the Eu^{3+} Ion in Complexes **1**−**3**

	spherical coordinates		
complex	R (Å)	θ (deg)	ϕ (deg)
1	2.389	95.260	3.929
HPBI oxygens	2.404	85.777	67.950
	2.403	22.177	317.905
	2.391	60.234	224.395
	2.408	126.109	135.354
	2.391	169.340	343.450
H_2O oxygens	2.394	62.246	130.176
	2.395	107.771	299.757
	2.392	119.730	215.772
2	2.394	90.263	359.162
HPBI oxygens	2.418	90.261	62.990
	2.401	49.447	281.445
	2.422	77.503	214.645
	2.397	123.386	279.665
	2.417	171.733	62.403
TOPO oxygens	2.326	25.919	113.968
	2.318	108.720	146.086
HPBI oxygens	2.411	93.019	356.070
	2.427	81.731	59.302
	2.427	73.579	271.379
	2.414	69.379	203.149
	2.421	153.617	47.562
	2.401	142.124	211.229
TPPO oxygens	2.327	94.362	130.858
	2.332	12.504	3.520
H_2O oxygen	2.399	124.246	300.250

(32) Pavithran, R.; Reddy, M. L. P. *Anal. Chim. Acta* **2005**, *536*, 219−226.

(33) Sabbatini, N.; Guardigli, M.; Manet, I. In *Handbook on the Physics and Chemistry of Rare Earth, 21*; Gschneidner, K. A., Jr., Eyring, L., Eds.; Elsevier Science BV: Amsterdam, The Netherlands, 1996; pp 69−119.

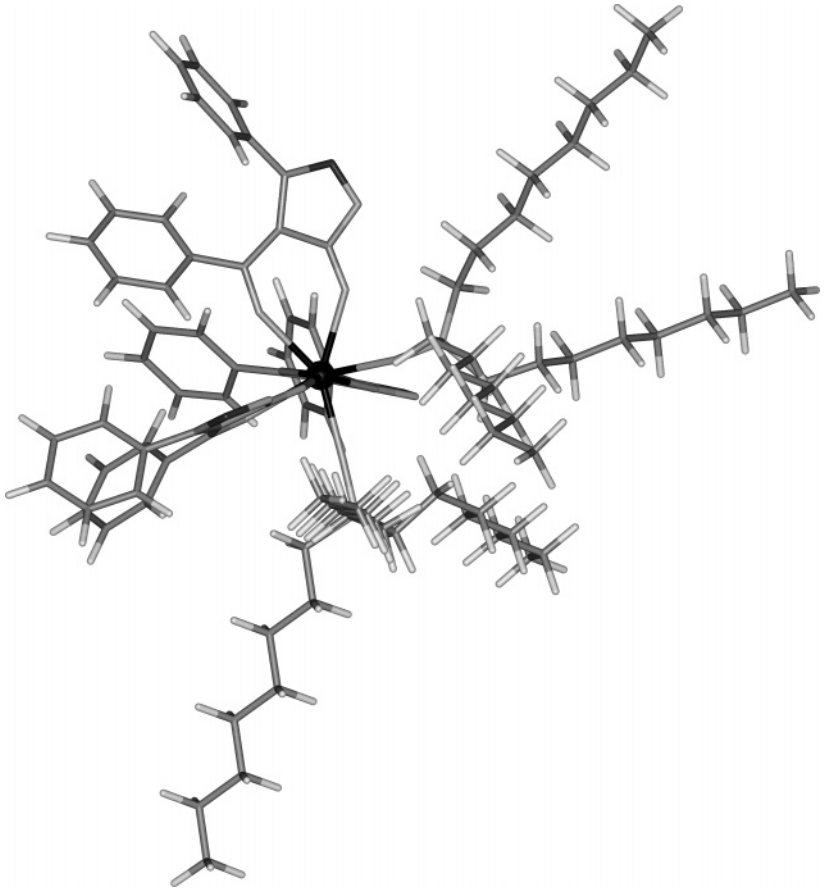

Figure 2. Optimized molecular structure of complex **2** obtained from the Sparkle/AM1 model.

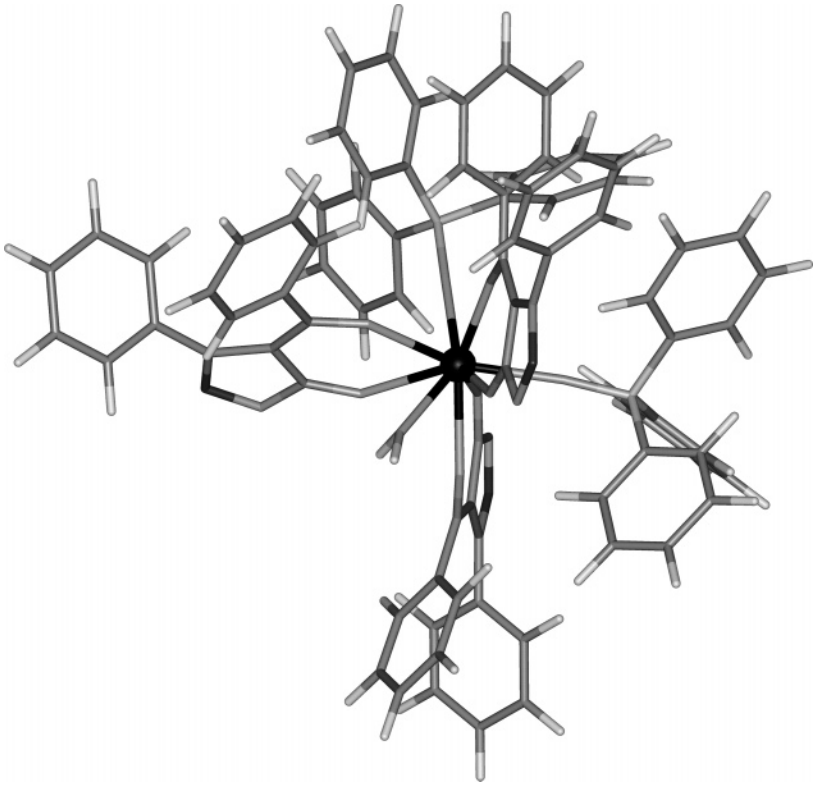

Figure 3. Optimized molecular structure of complex **3** obtained from the Sparkle/AM1 model.

of the ligand, has been observed, indicating that ET from the lowest triplet state of HPBI to the Eu^{3+} ion is efficient.

The lifetime values (τ) of the $^5D_0$ level were determined from the luminescence decay profiles for complexes **1**−**3** at

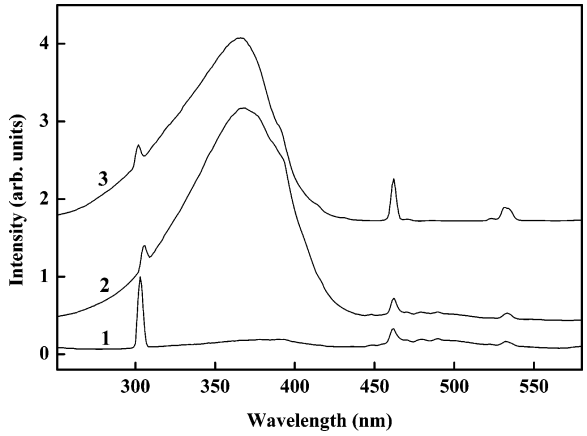

Figure 4. Excitation spectra of $^5D_0$ emission (λ_{max} = 614 nm) of Eu^{3+} in $Eu(PBI)_3 \cdot 3H_2O$ (**1**), $Eu(PBI)_3 \cdot 2TOPO$ (**2**), and $Eu(PBI)_3 \cdot 2TPPO \cdot H_2O$ (**3**) at 303 K.

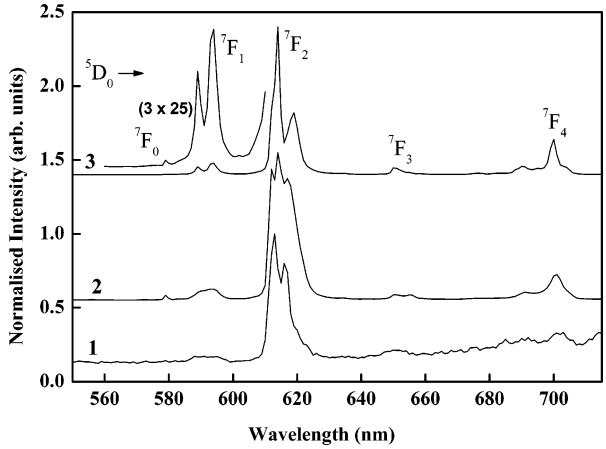

Figure 5. Room-temperature PL spectra of $Eu(PBI)_3 \cdot 3H_2O$ (**1**), $Eu(PBI)_3 \cdot 2TOPO$ (**2**), and $Eu(PBI)_3 \cdot 2TPPO \cdot H_2O$ (**3**) excited at 360 nm.

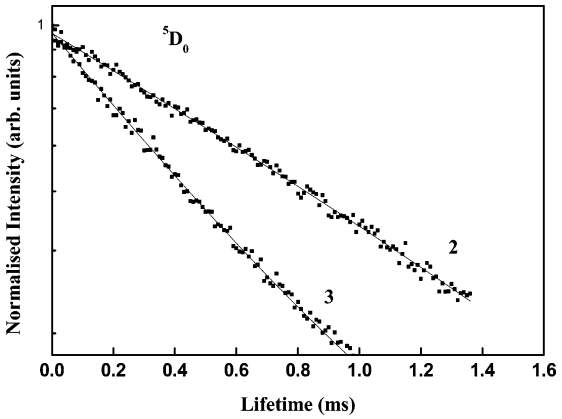

Figure 6. Experimental luminescence decay profiles of $Eu(PBI)_3 \cdot 2TOPO$ (**2**) and $Eu(PBI)_3 \cdot 2TPPO \cdot H_2O$ (**3**) excited at 360 nm and monitored at 612 nm.

room temperature by fitting with a monoexponential curve, and they are depicted in Table 2. Typical decay profiles of complexes **2** and **3** are shown in Figure 6. The relatively shorter lifetime obtained for complex **1** may be due to dominant nonradiative decay channels associated with vibronic coupling due to the presence of water molecules, as is well documented for many of the hydrated europium β-diketonate complexes.[8,27] A longer lifetime value has been observed for complex **2** as compared to complex **3**. This may also be due to the presence of a water molecule in complex **3**.

On the basis of the room-temperature emission spectra and on the lifetime measurements, we can estimate the emission quantum efficiency (η) of the $^5D_0$ europium ion excited state, considering that only nonradiative and radiative processes are essentially involved in the depopulation of the $^5D_0$ state.[1,10,34] The nonradiative rates, A_{NR}, can be obtained from the calculated rates, A_{RAD}, and the experimental decay rates by eq 8. A_{RAD} can be obtained by summation over the

$$1/\tau = A_T = A_{RAD} + A_{NR} \tag{8}$$

radiative rates A_{0J} for each $^5D_0 \rightarrow {}^7F_J$ transition.[1,10]

The emission quantum efficiency, η, can be expressed as

$$\eta = \frac{A_{RAD}}{A_{RAD} + A_{NR}} \tag{9}$$

Table 2 gives the A_{RAD}, A_{NR}, and quantum-efficiency values, η, for the $^5D_0$ europium ion excited state in complexes **1**−**3**. It is clear from Table 2 that complexes **1** and **3**, having water molecules in the coordination sphere, exhibit lower quantum efficiencies and lifetimes. This is due to the presence of O−H oscillators in these complexes, which effectively quench the luminescence of the Eu^{3+} ion. On the other hand, complex **2**, which does not have any water molecules in its coordination sphere, as is also evident from the molecular structure analysis by the Sparkle/AM1 model, exhibits high quantum-efficiency and lifetime values. The creation of lanthanide(III) complexes with higher emission yields is directly linked to the suppression of radiationless transitions caused by vibrational excitations in surrounding media.[13,35,36] Square-antiprismatic-structured europium complexes are expected to have increased radiation rates and quantum efficiencies because of increases in $^5D_0 \rightarrow {}^7F_2$ emissions (electronic dipole transitions), related to odd parity.[13] Thus, in the present study, complex **2** exhibits a high quantum efficiency as compared to complex **3**. Further, this quantum-efficiency value is found to be promising when compared to that observed for the various β-diketonate complexes of the Eu^{3+} ion involving Lewis bases (Table 3). The quantum efficiency measured for $Eu(tta)_3 \cdot 2DBSO$ (70%) is one of the highest so far reported for solid-state europium complexes.[8]

Judd−Ofelt analysis is a useful tool for estimating the population of odd-parity electron transitions.[38] Interaction parameters of ligand fields are given by the Judd−Ofelt

(34) Carlos, L. D.; Messaddeq, Y.; Brito, H. F.; Sa Ferreria, R. A.; de Zea Bermudez, V.; Ribeiro S. J. L. *Adv. Mater*. **2000**, *12*, 594−598.
(35) Wada, Y.; Ohkubo, T.; Ryo, M.; Nakarawa, T.; Hasegawa, Y.; Yanagida, S. *J. Am. Chem. Soc*. **2000**, *122*, 8583−8584.
(36) Hasegawa, Y.; Ohkubo, T.; Sogabe, K.; Kawamura, Y.; Wada, Y.; Nakashima, N.; Yanagida, S. *Angew. Chem., Int. Ed*. **2000**, *39*, 357−360.
(37) Fernandes, J. A.; Ferreira, R. A. S.; Pillnger, M.; Carlos, L. D.; Jepsen, J.; Hazell, A.; Ribeiro-Claro, P.; Goncalves, I. S. *J. Lumin*. **2005**, *113*, 50−63.
(38) Werts, M. H. V.; Jukes, R. T. F.; Verhoeven, J. W. *Phys. Chem. Chem. Phys*. **2002**, *4*, 1542−1548.

Table 2. Experimental Intensity Parameters, Radiative (A_{RAD}) and Nonradiative Decay Rates (A_{NR}), $^5D_0$ Lifetimes (τ), Quantum Efficiencies (η), and Calculated Singlet and Triplet Levels for Complexes **1**−**3** at 303 K

complex	$\Omega_2 \times 10^{-20}$ (cm^2)	$\Omega_4 \times 10^{-20}$ (cm^2)	A_{RAD} (s^{-1})	A_{NR} (s^{-1})	τ (ms)	η (%)	singlet (cm^{-1})	triplet (cm^{-1})
1	26.47	14.29	1059	2941	0.25	26	31 534	17 411
2	18.38	12.74	794	68	1.16	92	32 150	19 227
3	26.89	9.85	1002	921	0.52	52	32 346	19 224

Table 3. Solid-State Photophysical Data for $^5D_0$ Luminescence of Some Selected Eu^{3+} Complexes at Room Temperature[a]

complex	A_{RAD} (s^{-1})	A_{NR} (s^{-1})	lifetime τ (μs)	quantum efficiency (η)
$Eu(PBI)_3 \cdot 2TOPO$	794	68	1160	92
$Eu(tta)_3 \cdot Phen$[1]	436	993	700	31
$Eu(tta)_3 \cdot 2DBSO$[8]	980	420	1300	70
$Eu(btfa)_3 \cdot Phen$[8]	580	569	210	50
$Eu(btfa)_3 \cdot PhenNO$[8]	760	786	370	49
$Eu(NTA)_3 \cdot Phen$[37]	600	900	662	40

[a] tta = 2-thenoyltrifluoroacetonate; btfa = 4,4,4-trifluoro-1-phenyl-1,3-butanedionate; NTA = 1-(2-naphthoyl)-3,3,3-trifluoroacetonate; Phen =1,10-phenanthroline; Phen NO = phenanthroline *N*-oxide; DBSO = dibenzoyl sulfoxide.

parameters, Ω_λ. In particular, Ω_2 is more sensitive to the symmetry and sequence of ligand fields. To produce faster europium(III) radiation rates, antisymmetrical europium(III) complexes with larger Ω_2 parameters need to be designed. The experimental intensity parameters (Ω_λ, where $\lambda = 2$ and 4) were determined from the emission spectra for the Eu^{3+} ion given in Figure 5 based on the $^5D_0 \rightarrow {}^7F_2$ and $^5D_0 \rightarrow {}^7F_4$ transitions, with the $^5D_0 \rightarrow {}^7F_1$ magnetic-dipole-allowed transition as the reference, and they are estimated according to eq 10,[27,39] where A_{RAD} is the correspondent coefficient of

$$A_{RAD} = \frac{4e^2\omega^3}{3\hbar c^3}\chi\sum_\lambda \Omega_\lambda \langle {}^7F_J||U^{(\lambda)}||{}^5D_0\rangle^2 \frac{1}{2J+1} \qquad (10)$$

spontaneous emission, e is the electronic charge, ω is the angular frequency of the transition, $\hbar$ is Planck's constant over 2π, c is the velocity of light, and χ is the Lorentz local-field correction term, which is given by $n(n^2+2)^2/9$ with a refraction index $n = 1.5$, and $\langle {}^5D_0||U^{(2)}||{}^7F_J\rangle^2$ are the squared reduced matrix elements whose values are 0.0032 and 0.0023 for $J = 2$ and 4, respectively.[23] The Ω_6 parameter was not determined because the $^5D_0 \rightarrow {}^7F_6$ transition could not be experimentally detected. The Ω_2 and Ω_4 intensity parameters for complexes **1**−**3** at room temperature (300 K) are presented in Table 2. A point to be noted in these results is the relatively high values of Ω_2 for complexes **1**−**3**. This might be interpreted as being a consequence of the hypersensitive behavior of the $^5D_0 \rightarrow {}^7F_2$ transition.[40] The dynamic coupling mechanism is, therefore, dominant, indicating that the Eu^{3+} ion is in a highly polarizable chemical environment.

The ET rates from the ligand triplet state T to $^5D_1$ and $^5D_0$ levels and the ET rates from the singlet state S to $^5D_4$ level are presented in Table 4. We assumed a singlet → triplet intersystem cross rate of 10^8 s^{-1}, a triplet state decay rate of 10^5 s^{-1}, and a nonradiative decay rate of 10^6 s^{-1}.[8] Theoretical

Table 4. Predicted Values of Intramolecular ET Rates in the Complexes **1**−**3**[a]

complex	levels	transfer rate (s^{-1})	back-transfer rate (s^{-1})
1	$S_1 \rightarrow {}^5D_4$	9.486×10^5	6.862×10^{-3}
	$T \rightarrow {}^5D_1$	4.323×10^9	1.172×10^{13}
	$T \rightarrow {}^5D_0$	5.188×10^9	1.898×10^9
2	$S_1 \rightarrow {}^5D_4$	3.238×10^5	1.245×10^{-4}
	$T \rightarrow {}^5D_1$	3.333×10^9	1.577×10^9
	$T \rightarrow {}^5D_0$	2.376×10^9	1.518×10^5
3	$S_1 \rightarrow {}^5D_4$	1.508×10^7	2.277×10^{-3}
	$T \rightarrow {}^5D_1$	6.792×10^9	3.261×10^9
	$T \rightarrow {}^5D_0$	4.846×10^9	3.141×10^5

[a] The back-transfer rates were calculated by multiplying the direct transfer rates by the Boltzmann factor $e^{-|\Delta|/kT}$ at room temperature.

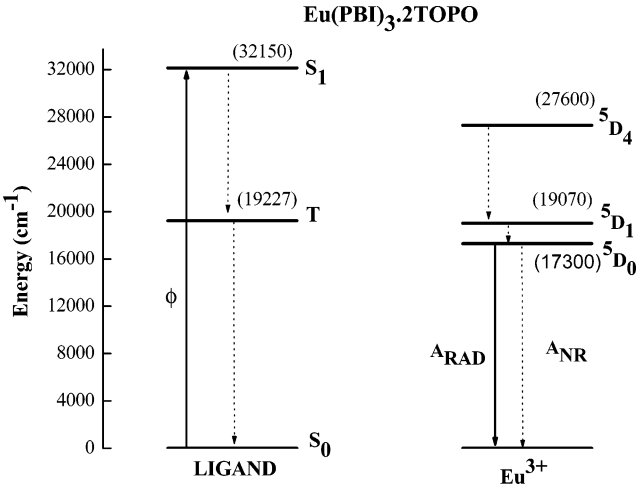

Figure 7. Energy level diagram of ligands and the Eu^{3+} ion in the $Eu(PBI)_3 \cdot 2TOPO$ complex.

energies of the singlet and triplet states were used in the calculation of the ET rates. We considered an average of the three singlet and triplet excited states, where the difference of the energy between the average values of the triplet states of the ^5D_J levels is smaller than 9.0 cm^{-1}. The average values of the singlet excited states were chosen because these values are closer to the values of the experimental singlet excited state of the complexes. The values for the theoretical triplet excited states were also chosen in the same way. An energy level diagram for the compound $Eu(PBI)_3 \cdot 2TOPO$ is shown in Figure 7. The symbols S_0, T, and S_1 shown in Figure 7 refer to the ground singlet, lowest energy triplet, and first excited singlet, respectively. The theoretical energies of the singlet and triplet were used in this diagram. According to the selection rules for the process of ET, in the case of the Eu^{3+} ion, levels $^5D_2$, $^5L_6$, $^5G_6$, and $^5D_4$ are good candidates for the multipolar mechanism, while for the exchange mechanism, a strong candidate is level $^5D_1$.[41] Then for the complexes in this work, the predominant process in the transfer of energy is the

(39) Malta, O. L.; dos Santos, M. A. C.; Thompson, L. C.; Ito, N. K. *J. Lumin.* **1996**, *69*, 77−84.
(40) Peacock, R. D. *Struct. Bonding* **1975**, *22*, 83−121.
(41) Malta, O. L. *J. Lumin.* **1997**, *71*, 229−236.

exchange mechanism. In accordance with Table 4, the values of the ET rate indicate that the ET from the triplet state of the ligand for the $^5D_1$ and $^5D_0$ levels of the Eu^{3+} ion is predominant.

Conclusions

Three new europium complexes, $Eu(PBI)_3 \cdot 3H_2O$ (**1**), $Eu(PBI)_3 \cdot 2TOPO$ (**2**), and $Eu(PBI)_3 \cdot 2TPPO \cdot H_2O$ (**3**), with different Lewis bases have been synthesized and characterized by various spectroscopic techniques. Their ground-state geometries have been calculated using the Sparkle/AM1 model. The characteristic emission spectra of Eu^{3+} complexes **1**−**3** show a very high intensity for the hypersensitive $^5D_0 \rightarrow {}^7F_2$ transition, pointing to a highly polarizable chemical environment around the Eu^{3+} ion. Theoretically predicted values of intramolecular ET rates of complexes **1**−**3** clearly indicate that the ET from the triplet state of the ligand to the $^5D_1$ and $^5D_0$ levels of the Eu^{3+} ion is predominant. It has been found that the $^5D_0$ quantum efficiency (η) and lifetime (τ) of the complexes vary considerably, depending on the nature of the adduct-forming ligand: TOPO ($\eta = 92\%$; $\tau = 1160$ μs), TPPO ($\eta = 52\%$; $\tau = 520$ μs), and H_2O ($\eta = 26$ %; $\tau = 250$ μs).

Higher quantum-efficiency and lifetime values observed for complex **2** than complexes **1** and **3** can be ascribed to a more efficient ligand-to-metal ET and less nonradiative $^5D_0$ relaxation process in the former case. The square-antiprismatic structure of europium complex **2** is also responsible for the increased radiation rates and high quantum efficiency. Further, the quantum-efficiency value observed in the present study, especially with complex **2** is found to be significantly higher than that so far reported for various β-diketonate complexes of the Eu^{3+} ion involving Lewis bases. Thus, our results demonstrate that the 3-phenyl-4-benzoyl-5-isoxazolonate complex of Eu^{3+} involving TOPO as the Lewis base may find potential application as emitting materials in the design of new light-conversion molecular devices.

Acknowledgment. The authors acknowledge financial support from the Council of Scientific and Industrial Research and Defence Research and Development Organization, India. The authors also thank Prof. T. K. Chandrashekar, Director, and Dr. Suresh Das, Head, Chemical Sciences Division, Regional Research Laboratory, Trivandrum, India, and Prof. C. K. Jayasanker, S.V. University, Tirupathi, India, for their constant encouragement and valuable discussions. They also acknowledge CENAPAD (Brazilian institution) for the computational facilities.

IC051781D